SIViP
DOI 10.1007/s11760-012-0298-0

ORIGINAL PAPER

Intracranial hemorrhage detection using spatial fuzzy c-mean and region-based active contour on brain CT imaging

H. S. Bhadauria · M. L. Dewal

Received: 4 December 2011 / Revised: 22 February 2012 / Accepted: 24 February 2012
© Springer-Verlag London Limited 2012

Abstract Intracranial hemorrhage (ICH) detection is the primary task for the patients suffering from neurological disturbances and head injury. This paper presents a segmentation technique that combines the features of fuzzy c-mean (FCM) clustering and region-based active contour method. In the suggested method, the fuzzy membership degree from FCM clustering is first used to initialize the active contour, which propagates for the detection of the desired object. In addition to active contour initialization, the fuzzy clustering is also used to estimate the contour propagation controlling parameters. The level set function as used by active contour in the proposed method does not need re-initialization process; thus, it fastens the convergent speed of the contour propagation. The efficacy of the suggested method is demonstrated on a dataset of 20 brain computed tomography (CT) images suffered with ICH. Experimental results show that the proposed method has advantages in accuracy in comparison with standard region growing method and FCM for the detection of hemorrhage from brain CT images.

Keywords Active contour method · Fuzzy c-mean (FCM) · Computed tomography (CT) · Intracranial hemorrhage (ICH)

1 Introduction

Intracranial hemorrhage (ICH) is one of the leading causes of death after heart disease and cancer in the world. It occurs as a result of bleeding due to leakage or rupturing of blood vessels within the brain substance. Due to this, hemorrhage detection entails as the primary task for the patients of the neurological disturbances and head injury. CT scans are widely used for the diagnosis of ICH. CT imaging not only provides experts an extraordinary way to diagnose the brain hemorrhage but it is also widely used due to its low cost, widespread availability, short imaging time, and excellent detection of bony details. The visualization of the hemorrhagic clot on brain CT images depends on its intrinsic properties like density, volume, location, relationship to surrounding structures, and technical factors like scanning angles and slice thickness [1]. Detection of hemorrhagic clot has crucial clinical significance because this may be useful in its prognosis and treatment trials. Intensity inhomogeneities and worst tissue contrast may cause considerable difficulties in the automatic hemorrhage detection from CT images. Lots of researches have been done on medical image segmentation, and two methods widely used are based on fuzzy set theory [2] and active contours [3]. In case of brain hemorrhage segmentation using CT images, Loncaric et al. [4,5] have largely contributed by using fuzzy c-mean (FCM) followed by rule-based classification of the regions. Chan [6] extracts the hemorrhagic region by using top-hat transform and left–right asymmetry. This system was capable of identifying small hemorrhagic clots. Bardera et al. [7] proposed a semi-automated segmentation method for brain hematoma and edema and also measures their volume. The method combines the region growing approach to segment the hematoma and level set segmentation to segment the edema. Liao et al. [8] proposed automatic intracranial hematoma detection technique based on multiresolution binary level set method. Zaki et al. [9] proposed an integrated system to extract the hemorrhage from brain CT images. The method used the multi-level FCM to extract an intracranial structure from its background and skull, and

H. S. Bhadauria (✉) · M. L. Dewal
Indian Institute of Technology, Roorkee, India
e-mail: hsb76iitr@gmail.com

M. L. Dewal
e-mail: mohanfee@iitr.ernet.in

Published online: 23 March 2012

then intracranial structure is segmented into cerebrospinal fluid, brain matter, and other homogenous matters using two-level Otsu multi-thresholding method. Further, hemorrhage detection carried by using symmetrical and pixel intensity features.

Active contour models are dynamic curves or surfaces that move within an image domain to capture desired object boundaries. The curve motion is driven by a combination of internal and external forces that achieve a minimal energy state when contour reaches the targeted object boundaries. There are two main mathematical approaches for the implementation of active contours: snakes and level sets. Snakes [10] explicitly move predefined snake points based on energy minimization scheme, while level set approaches [11] move contours implicitly as a particular level of a function. For image segmentation, active contour models can be classified into two classes viz. (i) edge-based models and (ii) region-based models. Edge-based models [12] use an edge detector, usually based on image gradient to attract the contour toward the desired object. Region-based active contour models identify the region of interest by using region descriptors to control the motion of contour. Chan and Vese [13] proposed region-based model for general images by minimizing Mumford–Shah functional [14]. By incorporating region-based information into the energy function, this method has much convergence range and flexible initialization. However, this model is computationally expensive and suffers from other difficulties.

In traditional active contour models, to keep the contour smooth, it is necessary to keep the evolving level set function close to signed distance function [15]. Thus, periodic re-initialization of level set function to signed distance function during evolution has been extensively used [16]. However, as shown by Gomes and Faugeras [17], re-initializing the level set function of active contour is a disagreement of the theory of the level set method and it is quite complicated, expensive, and has undesirable side effects. To overcome this problem, Li et al. [18] proposed a fast level set formulation, which forces the level set function closed to a signed distance function and thus eliminates the need of costly re-initialization process. In most of the active contour-based segmentation methods, the level set function is manually initialized. The presented work proposes an automated segmentation technique in which the fuzzy membership function from FCM clustering is first used to initialize the active contour, which propagates toward the boundaries of desired hemorrhagic region. In addition to automatic active contour initialization, the fuzzy clustering is also used to estimate the contour propagation controlling parameters.

Section 2 presents the methodology of the proposed fuzzy region-based active contour model to extract the hemorrhagic region from brain CT images. A brief description of fuzzy clustering and region-based active contour model is reproduced as the same are being used in the proposed method. The material and performance assessment parameters are discussed in Sect. 3. Section 4 presents the results and related observations with discussions followed by the conclusions in Sect. 5.

2 Methodology

The approach presented in the paper utilizes the features of both fuzzy clustering and region-based active contour model for automatic segmentation of hemorrhagic region from brain CT images. A brief introduction of spatial constrained fuzzy clustering and region-based active contour model is also given in Sects. 2.1 and 2.2, respectively. Section 2.3 presents the proposed approach.

2.1 Spatial fuzzy c-means clustering

FCMs clustering is an unsupervised technique that has been successfully used in medical image segmentation. An image can be represented in various feature spaces and FCM segments the image into objects by grouping the similar pixels in the feature space. The clustering is achieved by iterative minimization of a cost function that depends on the distance of the pixels to the cluster centers in the feature domain. Objective of image segmentation is to divide an image into meaningful regions. More formally, segmentation is a process of partitioning the entire image into c crisp maximally connected regions $\{R_i\}$ such that each R_i is homogeneous with respect to some criteria. In many situations, it is not easy to determine whether a pixel belongs to a region or not. To alleviate this situation, fuzzy set concepts can be used into the segmentation process. FCM [19] which has been widely used in medical image segmentation is one of the most popular algorithms in fuzzy clustering.

The standard FCM objective function for partitioning $\{x_k\}_{k=1}^{N}$ into c numbers of clusters is given by

$$J = \sum_{i=1}^{c} \sum_{k=1}^{N} u_{ik}^{m} \, \| x_k - v_i \|^2 \tag{1}$$

where x_k is the gray value of the kth pixel, v_i is the cluster center of the ith cluster, u_{ik} is the fuzzy membership of the kth pixel with respect to ith cluster, and m is the parameter controlling the fuzziness of the resultant segmentation. The fuzzy membership function is subjected to the following constraints.

$$\sum_{i=1}^{c} u_{ik} = 1 \, \forall \, k; \; u_{ik} \in [0, 1] \tag{2}$$

The membership function u_{ik} and cluster centers v_i can be calculated iteratively as

$$u_{ik} = \frac{\|x_k - v_i\|^{-2/m-1}}{\sum_{j=1}^{c} \left\|x_k - v_j\right\|^{-2/m-1}} \tag{3}$$

$$v_i = \frac{\sum_{k=1}^{N} u_{ik}^m x_k}{\sum_{k=1}^{N} u_{ik}^m} \tag{4}$$

FCM has been used with some success in medical image segmentation. However, since, the standard FCM does not consider any spatial information in image context, it suffers from the disadvantage of being sensitive to noise and other imaging artifacts. Recently, many researchers have incorporated local spatial information into the standard FCM. One of the important characteristics of an image is that the neighboring pixels are highly correlated, i.e., their probability of belonging to the same cluster gets high. Chuang et al. [20] utilized this spatial relationship and defined a spatial function as

$$h_{i,j} = \sum_{k \in NB(x_j)} u_{i,k} \tag{5}$$

where $NB(x_j)$ represents a square window centered on pixel x_j in the spatial domain. The spatial function is incorporated into membership function as follows

$$u'_{i,j} = \frac{u_{i,j}^p h_{i,j}^q}{\sum_{k=1}^{c} u_{k,j}^p h_{k,j}^q} \tag{6}$$

where p and q are parameters to control the contribution of both functions.

2.2 Region-based active contour model

Region-based active contours evolve deformable shapes based on two forces: energy minimization based on statistical properties, which pursue the uniformity and curvature motion motivated by level set function, which keeps the regularity of active contours. Starting with a contour around the object to be detected, the contour moves toward its interior normal and stops on the boundary of the object in the image. In level set formulation proposed by Osher and Sethian [11], the level set function $\varphi(x, y)$, which is two-dimensional Lipschitz function, represents the contour as $C = \{(x, y)/\varphi(x, y) = 0\}$ and evolution of this contour is given by zero level function $\varphi(t, x, y)$ at time t. The evolution equation of level set function φ is represented by following partial differential equation

$$\frac{\partial \varphi}{\partial t} = |\nabla \varphi| F, \quad \varphi(0, x, y) = \varphi_0(x, y) \tag{7}$$

where $\varphi_0(x, y)$ is the initial contour and F represents the speed function controlled by internal and external forces.

One of the biggest challenges in active contour models is that the level set function φ must be re-initialized periodically as a signed distance function. From the practical point of view, the re-initialization process can be quite complicated, expensive, and having side effects. In order to solve re-initialization problem, Li et al. [21] proposed new region-based model in which the re-initialization procedure is completely eliminated. In addition, in order to overcome the problems caused by intensity inhomogeneities, this method extracts the intensity information in local regions to guide the motion of the contour toward the desired object. This formulation is given as

$$\begin{aligned} \frac{\partial \varphi}{\partial t} = &-\delta_\varepsilon(\varphi)(\lambda_1 e_1 - \lambda_2 e_2) + \nu \delta_\varepsilon(\varphi) \operatorname{div}\left(\frac{\nabla \varphi}{|\nabla \varphi|}\right) \\ &+\mu\left(\nabla^2 \varphi - \operatorname{div}\left(\frac{\nabla \varphi}{|\nabla \varphi|}\right)\right) \end{aligned} \tag{8}$$

The first term is referred as the data fitting term and is responsible for propagating the active contour toward object boundaries. The second term is referred as length term and is responsible for smoothing of contour. The third term is called as level set regularization term since it maintains the regularity of the level set function close to signed distance function. λ_1 and λ_2 are weighting coefficients of data fitting term, ν is weighting coefficient of length term, and μ is the weighting coefficient of regularization term. $\delta_\varepsilon(x)$ is smoothed Dirac function, which is the derivative of smooth Heaviside function $H_\varepsilon(x)$. Both these functions are defined as

$$H_\varepsilon(x) = \frac{1}{2}\left[1 + \frac{2}{\pi}\tan^{-1}\left(\frac{x}{\varepsilon}\right)\right] \tag{9}$$

$$\delta_\varepsilon(z) = \frac{1}{\pi}\frac{\varepsilon}{\varepsilon^2 + x^2} \tag{10}$$

ε is a constant, which regularizes the Dirac function.

e_1 and e_2 are energy functions inside and outside the contour and defined as

$$e_1(x) = \int k_\sigma(y - x)\,|I(x) - f_1(y)|^2 \mathrm{d}y \tag{11}$$

and

$$e_2(x) = \int k_\sigma(y - x)\,|I(x) - f_2(y)|^2 \mathrm{d}y \tag{12}$$

f_1 and f_2 are data fitting functions centered at y and defined as

$$f_1(y) = \frac{K_\sigma * [H_\varepsilon(\varphi(y))I(y)]}{K_\sigma * H_\varepsilon(\varphi(y))} \tag{13}$$

and

$$f_2(y) = \frac{K_\sigma * [(1 - H_\varepsilon(\varphi(y)))I(y)]}{K_\sigma * (1 - H_\varepsilon(\varphi(y)))} \tag{14}$$

K_σ is the Gaussian kernel function and is defined as

$$K_\sigma(z) = \frac{1}{(2\pi)^{n/2}\sigma^n} e^{-|z|^2/2\sigma^2} \tag{15}$$

where $\sigma > 0$ is the standard deviation also known as scalar parameter.

In this formulation, the level set function $\varphi_0(x, y)$ is initialized as

$$\varphi_0(x, y) = \begin{cases} c, & (x, y) \in \Omega \\ -c, & (x, y) \notin \Omega \end{cases} \tag{16}$$

where c is a constant and should be larger than 2ε. Ω is the initial contour in which $\varphi_0(x, y) > 0$. The discretization of Eq. (8) can be expressed in the following iteration form

$$\varphi_{x,y}^{t+1} = \varphi_{x,y}^{t} + \tau \frac{\partial \varphi_{x,y}^{t}}{\partial t} \tag{17}$$

where τ is the time step parameter and can be taken sufficiently large. For maintaining the stable level set evaluation, the time step τ and penalty term μ must satisfy $\tau \cdot \mu < 1/4$.

2.3 The proposed fuzzy-based level set segmentation method

The proposed approach utilizes the features of both fuzzy clustering and region-based active contour method to the automatic segmentation of hemorrhagic region from brain CT images. The method first segments the hemorrhagic area using fuzzy clustering. At this stage, it is worthwhile to notice that the fuzzy clustering generates spurious blobs and outliers in the image. The morphological operations viz. erosion and dilation have been used to get rid of these side effects. The erosion shrinks and removes the spurious blobs and outliers, and dilation expands and recovers the object of interest.

After having performed the stated morphological operations, the results of fuzzy clustering are used to initialize the level set function as well as to estimate the controlling parameters, which control the evolution of level set function. Let $U_{i,j} = [u_{i,j}]$ be the membership function for the fuzzy segmentation. The object of interest from the given image can be extracted as binary image $Z_{i,j}$

$$Z_{i,j} = \begin{cases} 1, & u_{i,j} \geq b_0 \\ 0, & \text{otherwise} \end{cases} \tag{18}$$

$b_0 \in (0, 1)$ is the adjustable threshold.

Now, the level set function can be initialized as

$$\varphi_0(x, y) = 2\varepsilon(2Z_{i,j} - 1) \tag{19}$$

where ε is a constant that regularizes the Dirac function as given Eq. (12).

In traditional level set methods, several controlling parameters which control the level set evolution are manually inputted and their values vary from case to case. In the proposed method, all these controlling parameters are adaptively estimated from the results of fuzzy clustering. The area and length of the contour produced by fuzzy clustering are computed using Heaviside function and Dirac function as

$$C_{\text{Area}}(\varphi \geq 0) = \int_\Omega H(\varphi(x, y))\mathrm{d}x\mathrm{d}y \tag{20}$$

$$C_{\text{length}}(\varphi = 0) = \int_\Omega \delta_0(\varphi(x, y))\,|\nabla\varphi(x, y)|\mathrm{d}x\mathrm{d}y \tag{21}$$

where Heaviside function is defined as

$$H(\varphi) = \begin{cases} 1, & \text{if } \varphi \geq 0 \\ 0, & \text{if } \varphi < 0 \end{cases} \tag{22}$$

and the Dirac function as

$$\delta_0(\varphi) = \frac{\mathrm{d}}{\mathrm{d}\varphi} H(\varphi) \tag{23}$$

As mentioned by Li et al. [18], time step of level set evolution τ in Eq. (17) can be chosen sufficiently large and the product of time step τ and regularization term coefficient μ must satisfied the condition $\tau \cdot \mu < 1/4$ for stable evolution. The time step parameter τ is estimated as

$$\tau = \frac{C_{\text{Area}}}{C_{\text{Length}}} \tag{24}$$

The regularization term coefficient μ is estimated as

$$\mu < \frac{1}{4\tau} \tag{25}$$

The first term in Eq. (8) speeds up the attraction of the level set function toward the desired object. This term consists of two weighting coefficients λ_1 and λ_2, over the region outside and inside the contour C, respectively. The value of these weights should be same to lead the fair

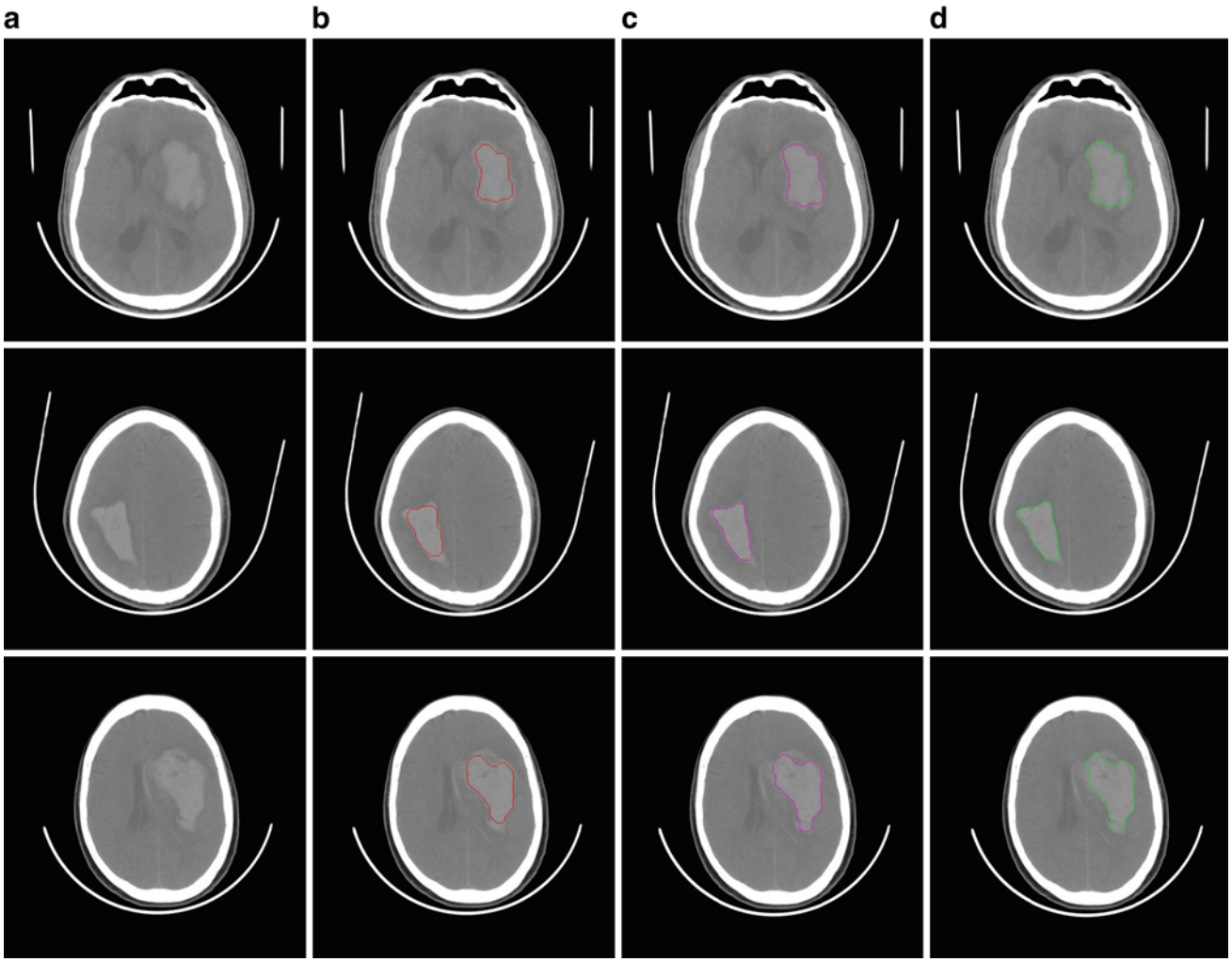

Fig. 1 ICH detection: column (**a**) original CT images (**b**) region growing method (**c**) fuzzy clustering method (**d**) proposed method

competition between the regions inside and outside the contour during the evolution. Thus, in the proposed approach, the value of λ_1 and λ_2 is estimated from the results of fuzzy clustering as

$$\lambda_1 = \lambda_2 = 0.5 - u_{i,j} \tag{26}$$

where $u_{i,j}$ is the membership function value for the fuzzy clustering at each pixel of the image.

The second term in Eq. (8) is responsible for smoothing the contour. In the proposed approach for achieving the smoother contour, the value of ν is estimated as

$$\nu = 0.2\tau \tag{27}$$

3 Material and performance evaluation parameters

To evaluate the performance of proposed segmentation method, a dataset of 20 CT images suffering with ICH has been taken. These brain CT images are acquired from CT scanner manufactured by General Electric (GE) medical systems. All the images are scanned parallel to the orbitomeatal line (OML) with the exposure of peak tube voltage and tube current as 120 kV and 100 mA, respectively. Each image is having the field of view (FOV) 25 × 25 cm and the size 512 × 512, resulting the resolution of 0.49 × 0.49 mm^2 per pixel. The thickness of the slices is 10 mm throughout the brain. The original CT numbers are converted into 256 gray levels with brain window parameters as center 40 and width 400.

The manually delineated hemorrhage region drawn by an expert is taken as the ground truth and compared with the results of proposed segmentation technique. The performance of the proposed segmentation technique is evaluated using four quantitative parameters like sensitivity, specificity, Jaccard index, and Dice coefficients. Sensitivity means percentage of hemorrhagic pixels properly included in segmentation results out of all the pixels in the results of

Table 1 Comparison between different hemorrhage detection methods from brain CT images

CT scan no.	Hemorrhagic area (cm^2)						
	Manually delineated (a)	Region growing (b)	Difference (a–b)	Fuzzy clustering (c)	Difference (a–c)	Proposed method (d)	Difference (a–d)
1	13.09	11.12	1.97	12.14	0.95	12.54	0.55
2	1.72	1.22	0.5	1.42	0.3	1.48	0.24
3	11.52	7.18	4.34	9.65	1.87	9.94	1.58
4	16.62	12.7	3.92	13.43	3.19	14.78	1.84
5	12.46	9.16	3.3	10.64	1.82	10.86	1.6
6	15.48	13.95	1.53	13.85	1.63	14.45	1.03
7	11.87	7.97	3.9	9.42	2.45	9.64	2.23
8	10.78	8.62	2.16	8.99	1.79	9.55	1.23
9	11.08	7.74	3.34	9.25	1.83	9.6	1.48
10	10.14	8.82	1.32	8.62	1.52	9.45	0.69
11	12.52	8.22	4.3	10.63	1.89	10.93	1.59
12	10.87	6.97	3.9	8.42	2.45	8.64	2.23
13	11.4	8.16	3.24	9.6	1.8	9.86	1.54
14	12.09	8.74	3.35	10.24	1.85	10.54	1.55
15	15.62	11.65	3.97	12.35	3.27	13.73	1.89
16	14.09	10.01	4.08	13.15	0.94	13.54	0.55
17	9.78	6.58	3.2	7.99	1.79	8.57	1.21
18	10.12	8.82	1.3	8.69	1.43	9.34	0.78
19	15.44	13.95	1.49	13.83	1.61	14.39	1.05
20	1.58	1.18	0.4	1.32	0.26	1.45	0.13
Average	11.41	8.64	2.78	9.68	1.73	10.16	1.25

segmentation. Specificity means percentage of hemorrhagic pixels properly excluded from the segmentation results out of all the pixels outside of ground truth hemorrhage. These parameters are defined as follows:

$$\%\ \text{Sensitivity} = \left(\frac{\text{TP}}{\text{TP} + \text{FN}}\right) * 100 \tag{28}$$

$$\%\ \text{Specificity} = \left(\frac{\text{TN}}{\text{TN} + \text{FP}}\right) * 100 \tag{29}$$

TP or true positive means a pixel appearing in both manually segmented hemorrhage area and hemorrhage area detected by computerized method. TN or true negative means a pixel absent in both manually segmented hemorrhage area and hemorrhage area detected by computerized method. FP or false positive means a pixel absent in manually segmented hemorrhage area but it appears in hemorrhage boarder detected by computerized method. FN or false negative means a pixel appearing in the manually segmented hemorrhage boarder but it is absent from hemorrhage boarder detected by computerized method [22].

Jaccard index is a statistical measure of similarity between sample sets. For the two sets, it is defined as the cardinality of their intersection divided by the cardinality of the union.

$$\text{JaccardIndex} = \frac{R_{\text{GT}} \cap R_{\text{CS}}}{R_{\text{GT}} \cup R_{\text{CS}}} \tag{30}$$

$$\text{DiceCoefficient} = 2 * \frac{R_{\text{GT}} \cap R_{\text{CS}}}{R_{\text{GT}} + R_{\text{CS}}} \tag{31}$$

where R_{GT} represents manually segmented ground truth hemorrhage region and R_{CS} represents hemorrhage area detected by the computerized method.

4 Experimental results and discussions

ICH detection from brain CT images is the challenging task due to its weak and irregular boundaries. To validate the usefulness of the proposed method, a variety of brain CT images, suffered with ICH of different sizes and shapes is acquired. The results are compared with standard region growing and fuzzy clustering-based segmentation methods. From Fig. 1, it can be observed that the proposed method extracts the hemorrhagic regions and boundaries with the highest accuracy. For further analysis of the results, the hemorrhagic regions are manually delineated by the subject expert and taken as ground truth. Table 1 shows the area of hemorrhagic regions extracted using different methods and their comparative

Table 2 Sensitivity and specificity analysis of hemorrhage detection methods on brain CT images

Image no.	Sensitivity			Specificity		
	Region growing	Fuzzy clustering	Proposed method	Region growing	Fuzzy clustering	Proposed method
1	74.79	78.85	86.96	98.67	99.93	99.98
2	85.63	85.18	90.36	97.74	99.13	98.37
3	58.95	75.63	76.49	99.66	99.52	99.93
4	76.89	77.25	77.76	99.67	99.68	99.47
5	65.24	71.92	72.35	90.62	86.89	100
6	62.20	73.46	74.52	99.45	99.94	99.97
7	82.84	84.56	87.27	99.65	99.72	99.74
8	64.91	77.73	80.59	99.64	99.23	100
9	58.86	76.17	78.74	96.45	92.29	96.89
10	57.89	68.84	69.85	99.56	100	100
11	62.20	73.16	74.57	99.40	99.93	99.98
12	57.89	67.84	69.45	99.59	100	100
13	74.59	78.95	86.56	98.66	99.91	99.97
14	62.18	71.02	72.30	90.60	86.89	100
15	58.90	74.75	76.49	99.76	99.55	99.91
16	53.86	78.17	79.76	96.47	92.20	96.88
17	85.53	85.01	90.06	97.75	99.12	98.36
18	83.81	84.58	87.21	99.68	99.71	99.71
19	76.61	77.15	77.86	99.57	99.58	99.27
20	60.83	77.77	80.49	99.64	99.09	100
Average	68.23	76.90	79.48	98.11	97.62	99.42

Table 3 Jaccard index and Dice coefficients for hemorrhage detection methods on brain CT images

Image no.	Jaccard Index			Dice coefficients		
	Region growing	Fuzzy clustering	Proposed method	Region growing	Fuzzy clustering	Proposed method
1	0.8256	0.8687	0.9142	0.8642	0.8810	0.9214
2	0.8452	0.8467	0.8708	0.9144	0.9149	0.9326
3	0.6885	0.7432	0.7611	0.7429	0.8534	0.8606
4	0.7626	0.7682	0.7742	0.8644	0.8687	0.8732
5	0.6288	0.6319	0.6509	0.7768	0.7814	0.8059
6	0.6420	0.7214	0.7416	0.7769	0.8448	0.8517
7	0.8359	0.8424	0.8673	0.9125	0.9175	0.9310
8	0.6582	0.7763	0.8025	0.7665	0.8715	0.8966
9	0.5524	0.7599	0.7750	0.7063	0.8405	0.8624
10	0.5887	0.6782	0.6926	0.7343	0.8054	0.8176
11	0.6219	0.7311	0.7413	0.7669	0.8447	0.8514
12	0.5789	0.6784	0.6916	0.7333	0.8084	0.8177
13	0.7456	0.7888	0.8541	0.8543	0.8819	0.9213
14	0.6218	0.6279	0.6609	0.7668	0.7714	0.7959
15	0.5885	0.7441	0.7631	0.7409	0.8533	0.8656
16	0.5224	0.7399	0.7550	0.6863	0.8505	0.8604
17	0.8415	0.8427	0.8808	0.9140	0.9146	0.9366
18	0.8357	0.8434	0.8693	0.9105	0.9150	0.9301
19	0.7606	0.7682	0.7752	0.8640	0.8689	0.8734
20	0.6083	0.7707	0.8020	0.7565	0.8705	0.8901
Average	0.6877	0.7586	0.7822	0.8026	0.8579	0.8748

evaluation with respect to the hemorrhagic regions manually delineated by an expert. The approximate hemorrhagic areas detected by proposed method range from 1.45 to 14.78 cm^2 with an average of 10.16 cm^2 for 20 brains CT image dataset. The average of difference of hemorrhagic area detected by standard region growing and fuzzy clustering with respect to manually delineated region by an expert are 2.78 and 1.73, respectively, whereas similar value detected by the proposed method is 1.25, which is the minimum and the evidence of highest accuracy of proposed method. The quantitative evaluation of the segmentation results in terms of similarity indices like sensitivity, specificity, Jaccard index, and Dice coefficients are also calculated and collated in Tables 2 and 3. From Table 2, it can be shown that for the proposed method, sensitivity ranges from 69.45 to 90.36 with an average value of 79.48 and specificity ranges from 96.88 to 100 with an average value of 99.44. For further validation, Jaccard index and Dice coefficients are also computed and shown in Table 3. For the proposed method, Jaccard index ranges from 0.6509 to 0.9142 with an average value of 0.7822 and the Dice coefficients range from 0.7959 to 0.9366 with an average value of 0.8748. It can be observed from Tables 2 and 3 that the average values of all similarity indices are highest in case of proposed method, which indicates that the results of the proposed method correlates well within the expert's measurements.

5 Conclusion

The identification of ICH is one of the vital most tasks because of the high morbidity and mortality rate on its count. It is the least treatable form of stroke and the measurement of its area from brain CT images is immediately useful for prognosis and treatment trials. This paper proposes an automatic hemorrhage segmentation technique for brain CT images, which utilizes the fuzzy clustering to initialize the level set function and, in addition to this, it estimates the level set evolution controlling parameters automatically. The experimental results show that the proposed method is much robust and accurate for the detection of hemorrhagic region. The results corroborate well within the measurements made by the experts, showing that the proposed method may be used for clinical purposes.

References

1. Cohen, W., Wayman, L.: Computed tomography of intracranial hemorrhage. Neuroimaging Clin. N Am. **2**, 75–87 (1992)
2. Pham, D.L., Prince, J.L.: An adaptative fuzzy segmentation algorithm for three dimensional magnetic resonance images. Information processing in medical imaging (IPMI), 140–153 (1999)
3. Caselles, V., Catte, F., Coll, T., Dibos, F.: A geometric model for active contours in image processing. Numerische Mathematik **66**, 1–31 (1993)
4. Loncaric, S., Dhawan, A.P., Kovacevic, D., Cosic, D., Broderick, J., Brott, T.: Quantitative intracerebral brain hemorrhage analysis. In: Proceedings of SPIE Medical Imaging, vol. 3661, pp. 886–894 (1999)
5. Loncaric, S., Kovacevic, D., Cosic, D.: Fuzzy expert system for edema segmentation. In: Proceedings of the IEEE 9th Mediterranean Electro-Technical Conference, pp. 1476–1479 (1998)
6. Chan, T.: Computer aided detection of small acute intracranial hemorrhage on computer tomography of brain. Int. J. Comput. Med. Imaging Graph. **31**, 285–298 (2007)
7. Bardera, A., Boada, I., Feixas, M., Remollo, S., Blasco, G., Silva, Y., Pedraza, S.: Semi-automated method for brain hematoma and edema quantification using computed tomography. Int. J. Comput. Med. Imaging Graph. **33**, 304–311 (2009)
8. Liao, C.C., Xiao, F., Wong, J.M., Chiang, I.J.: Computer aided diagnosis of intracranial hematoma with brain deformation on computed tomography. Int. J. Comput. Med. Imaging Graph. **34**, 563–571 (2010)
9. Zaki, W., Fauzi, M., Besar, R., Ahamad, W.: Abnormalities detection in serial computed tomography brain images using multilevel segmentation approach. J. Multimedia Tools Appl. **54**, 321–340 (2011)
10. Kass, M., Witkin, A., Terzopoulos, D.: Snakes: active contour models. Int. J. Comput. Vis. **1**, 321–331 (1987)
11. Osher, S., Sethian, J.A.: Fronts propagating with curvature dependent speed: algorithms based on Hamilton-Jacobi formulations. J. Comput. Phys. **79**, 12–49 (1988)
12. Caselles, V., Kimmel, R., Sapiro, G.: Geodesic active contour. Int. J. Comput. Vis. **22**, 61–79 (1997)
13. Chan, T., Vese, L.: Active contours without edge. In: IEEE Trans. Image Process. **10**, 266–277 (2001)
14. Mumford, D., Shah, J.: Optimal approximation by piecewise smooth functions and associated variational problems. Commun. Pure Appl. Math. **42**, 577–685 (1989)
15. Peng, D., Merriman, B., Osher, S., Zhao, H., Kang, M.: A PDE-based fast local level set method. J. Comput. Phys. **155**, 410–438 (1999)
16. Osher, S., Fedkiw, R.: Level Set Methods and Dynamic Implicit Surfaces. Springer, New York (2002)
17. Gomes, J., Faugeras, O.: Reconciling distance functions and level set. J. Vis. Commun. Image Represent. **11**, 209–223 (2000)
18. Li, C., Xu, C., Gui, C., Fox, M.D.: Level set evolution without re-initialization: a variational formulation. In: Proceedings of IEEE Conference Computer Vision and Pattern Recognition, pp. 430–436 (2005)
19. Bezdek, J.C., Pal, S.K.: Fuzzy Models for Pattern Recognition. In: IEEE Press, Piscataway (1991)
20. Chuang, K.S., Tzeng, H.L., Chen, S., Wu, J., Chen, T.J.: Fuzzy c-means clustering with spatial information for image segmentation. Comput. Med. Imaging Graph. **30**, 9–15 (2006)
21. Li, C., Kao, C.Y., Gore, J.C., Ding, Z.: Minimization of region-scalable fitting energy for image segmentation. In: IEEE Trans. Image Process. **17**(10), 1940–1949 (2008)
22. Metz, C.: Basic principles of ROC analysis. Semin. Nucl. Med. **8**, 283–298 (1978)